

## Comparison of Heat-Properties and its Implications between Standard-Oil and Bio-Oil

### Marcel Rückert

RWTH Aachen University, Institute for Fluid Power Drives and Controls (IFAS), Aachen, Germany, E-mail: [marcel.rueckert@ifas.rwth-aachen.de](mailto:marcel.rueckert@ifas.rwth-aachen.de)

### Dr.-Ing. Katharina Schmitz

Walter Hunger International GmbH, Alfred-Nobel-Str. 26, 97080 Würzburg, Germany, E-mail: [K.Schmitz@hunger-international.de](mailto:K.Schmitz@hunger-international.de)

### Professor Dr.-Ing. Hubertus Murrenhoff

RWTH Aachen University, Institute for Fluid Power Drives and Controls (IFAS), Aachen, Germany, E-mail: [post@ifas.rwth-aachen.de](mailto:post@ifas.rwth-aachen.de)

### Abstract

An important criteria for optimising hydraulic systems is their size. Especially for tanks and heat exchangers oil parameters as heat capacity and thermal conductivity have a big influence on the size. Additionally, various oils differ in their parameters. Accordingly, the heat capacity and thermal conductivity need to be known. However, little research has been done. Data-sheets usually do not provide any thermal data.

In this paper, the thermal conductivity is measured for varying types of hydraulic oils. The thermal conductivity is determined by a newly designed test-rig measuring the radial temperature difference in a tube at a quasi-static state using a constant heat flux. Thus, an overview over the thermal conductivity of different oils is achieved. Based on the results, a comparison between different types of fluid is made.

**KEYWORDS:** Bio-Oil, Thermal Conductivity, Mineral-Oil, Thermal Properties

### 1. Introduction

Thermodynamic measuring is strongly dependent on the data available. Witt proposed a model in order to describe thermal effects on viscosity and density of different oils using model equations, /1/. Additionally, he derived a model to describe the hydraulic efficiency using thermodynamic measurements. One of the properties which hasn't been subject of research is the thermal conductivity.

An investigation of the efficiency of an external gear pump as a function of the temperature has been discussed by Lana et al. in [2]. Within this study, a thermodynamic model has been derived and assessed under the experimental and simulative point of view. Additionally, the pump structure has been artificially worn and the influence of the wear on efficiency has been investigated. In the proposed model by, the thermal conductivity is necessary in order to calculate the hydraulic efficiency.

Assuming an incompressible flow, the first law of thermodynamics for a pump can be written as in (1), where  $\Delta T$  is the difference between the up- and downstream temperature. On the right hand side,  $\beta$  is the coefficient of thermal expansion and  $v$  is the specific volume of the fluid. Finally,  $P$  and  $\dot{Q}$  describe the input shaft power and the heat flux through the pump housing respectively. The latter is given in (2), which is the heat transfer through the surfaces of the pump housing to the surrounding. In order to compute such heat flux, (2) utilises the difference between the average fluid temperature  $\bar{T}$  and the surrounding temperature  $T_s$ , the heat transfer coefficient  $h_s$  and the net exchange surface  $A_s$ .

$$\Delta T = \frac{\dot{Q} - P}{\rho Q \bar{c}_p} - \frac{(1 - \beta \bar{T}) \bar{v} \Delta p}{\bar{c}_p} \quad (1)$$

$$\dot{Q} = \bar{h}_e A_s (\bar{T} - T_u) \quad (2)$$

Both equations (1) and (2) are defined for a steady state of the system. For this reason, a homogeneous and isotropic temperature is assumed in. **Figure 1** shows the comparison between the theoretical results and the experimental ones for an external gear pump at a rotational speed of 1750 1/min.

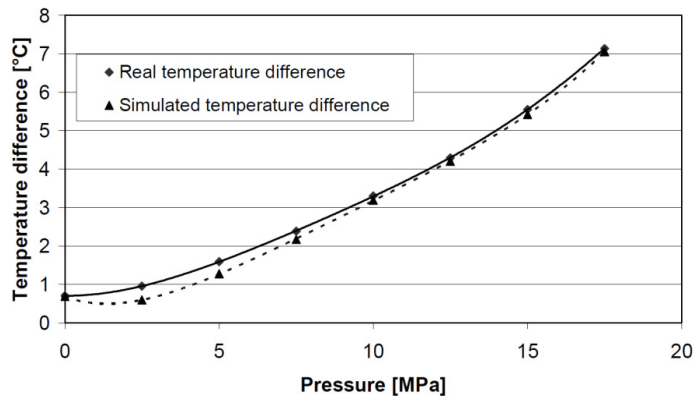


**Figure 1:** Measured and simulated temperature difference of the in- and outlet of an external gear pump [2]

Next to practical applications, multi-dimensional system simulations also require accurate data, especially when considering CFD simulations. The modelling of the fluid requires detailed information on the thermal properties in order to make precise predictions. Unfortunately, modelling the thermal properties of the fluid is a difficult task, because of lack of data. Especially the thermal conductivity is a parameter that can influence simulation results.

## 2. Introduction into Thermal Conductivity

In order to calculate the heat flux in (2), it is necessary to possess data regarding the thermal conductivity of the oil used.

The heat flux describes the transport of thermal energy by atomic and molecular interactions. Assuming a body to be homogeneous and isotropic, a temperature difference within the body leads to a heat flux which is independent from other effects. By normalising the heat flux in respect to the cross section area the heat flux density can be defined. According to Fourier there is a proportional relationship between heat flux density and temperature gradient, see (3) and /3/.

$$q'' = -\lambda \cdot \text{grad } T \quad (3)$$

The factor for the proportional relationship between the heat flux density and the temperature gradient is called thermal conductivity  $\lambda$ . The thermal conductivity of oils at 20 °C is shown in **Table 1**.

Oil	HLP46	HETG
$\lambda$	0.14	0.17

**Table 1:** Literature Data for HLP and HETG at 20 °C /4/

For a one-dimensional case the heat flux depends on the distance between two points, the temperature difference across it and the thermal conductivity of the material in between. In **Figure 2** The area normalised heat flux or heat flux density  $\dot{q}''$  enters at the first test point and exits at the second test point in a distance  $\delta$ . This leads to a temperature difference between the first test point temperature  $T_i$  and the second test point temperature  $T_a$ . By using equation (4), the heat flux density, the temperature difference and the distance define the thermal conductivity. This one-dimensional case is valid for two large but thin plates touching each other. When heating one of them, the other gets warmer too. Additionally, the effects on the edges of the plates are negligible.



**Figure 2:** Thermal Conductivity in 1D

$$\dot{q}'' = \lambda \cdot \frac{T_i - T_a}{\delta} \quad (4)$$

An example for a two-dimensional case is a long but thin pipe with a centric heat source. Here the distance between two measurement points is in radial direction. Due to the changing cross section for the heat flux with changing radius, the temperature profile is not linear any more. Instead it has a logarithmic shape, according to (5) and deduced in /5/. A sketch for a two-dimensional case is shown in **Figure 3**. The two-dimensional approach assumes that effects at the end of the pipe can be neglected.

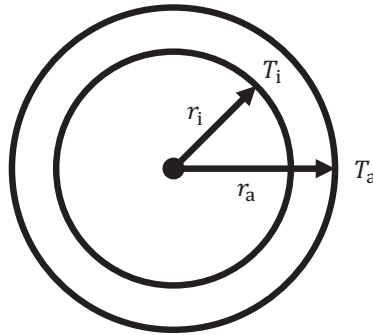


**Figure 3:** Thermal Conductivity in 2D

$$\dot{q}'' = \lambda \cdot \frac{T_i - T_a}{\ln(r_a/r_i)} \quad (5)$$

When considering the heat transfer within fluids two effects occur. First the thermal conductivity as explained above leads to a heat transfer. However, due to the motion of the fluid convection might lead to further heat transfer. The separation of both effects is difficult in measurement. Thus the Rayleigh number  $Ra$  is used to estimate the extent of the convection. It is defined by Grashof number  $Gr$  and Prandtl number  $Pr$ , see (6), and describes the relationship between lifting forces and viscosity forces for a temperature difference applied. In case of the Rayleigh number  $Ra \ll 1000$  the convection can be neglected. This is valid for the test rig explained later for temperatures below 500 K, compare with /5/.

$$Ra = Gr \cdot Pr \quad (6)$$

Another heat transport mechanism is thermal radiation. Because of the low thermal conductivity of oil and the resulting low temperature differences, radiation can be neglected for the planned test rig.

### 3. Thermal Conductivity Test Rig

The principal idea of the thermal conductivity test rig is to create a closed volume that can be compressed in order to adjust the pressure to a desired level. Additionally, a defined heat flow can be introduced and the radial temperature difference can be measured at various positions. The measurement principle can be seen in **Figure 4**. Temperature sensors are located at varying radial distances around a centric heat source. Through a heat wire a heat flux  $\dot{Q}$  is introduced. With the electric resistance  $R$  of the heat wire and the current  $I$ , the heat flux can be calculated using (7).

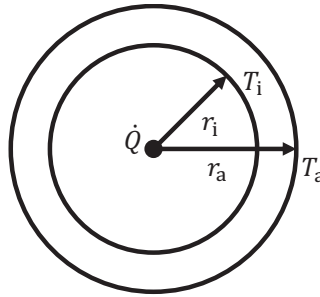


**Figure 4:** Radial Heat Flow

In order to derive the thermal conductivity, (8) can be expanded by the length of the wire  $L$ . After solving for  $\lambda$ , (9) shows the final equation to calculate the thermal conductivity for the test rig.

$$\dot{Q} = U \cdot I = R \cdot I^2 \quad (7)$$

$$\dot{Q} = \lambda L \cdot \frac{\Delta T}{\ln\left(\frac{r_a}{r_i}\right)} \quad (8)$$

$$\lambda = \frac{\dot{Q}}{L} \cdot \frac{\ln\left(\frac{r_a}{r_i}\right)}{\Delta T} = \frac{R \cdot I^2}{L} \cdot \frac{\ln\left(\frac{r_a}{r_i}\right)}{\Delta T} \quad (9)$$

**Figure 5** shows a sectional view of the conceptual design of the test rig. The housing consists of a steel pipe and an end cap. The end cap (left) can be moved to adjust the volume. By torquing tie rods the volume and thus various pressures can be applied.

Four sensors are used. The first one is the pressure sensor, the other three are temperature sensors. Their measuring heads are positioned in different distances to the sensors landing, while the sensors are mounted in a row parallel to the test rig's axis.

Through a thread opposite to the end cap the heating wire is integrated. When applying an electric voltage to the wire current flows heating it. Various voltages and thus powers can be provided by the power-supply unit used. The alignment of the wire is ensured by tightening it with a hook integrated in the end cap. The hook is mounted on a spring providing a tightening force despite different end cap positions. Thus a centric and straight position is achieved for all operation points.

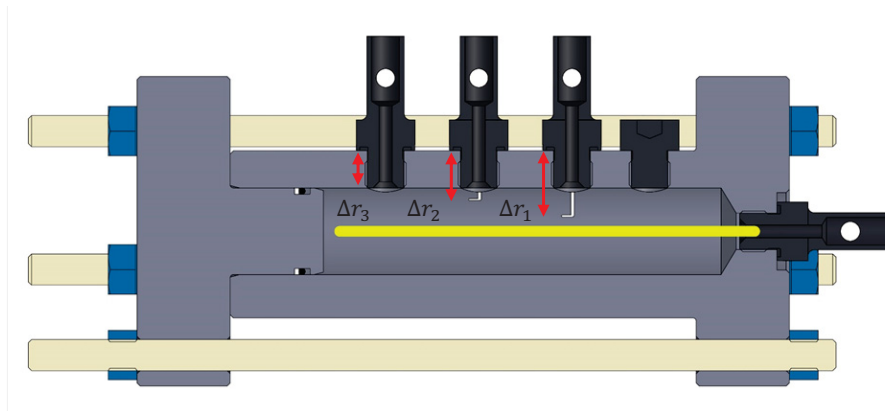


**Figure 5:** Conceptual Design of the Test Rig

For measurement the wire is heated with the power-supply unit. A defined power is provided. This electric power is converted into heat leading to a heat flow and thus a radial temperature gradient in the oil. Due to the different radial positions of the temperature sensors, this temperature gradient can be measured, see **Figure 6** showing the schematics of the test rig.

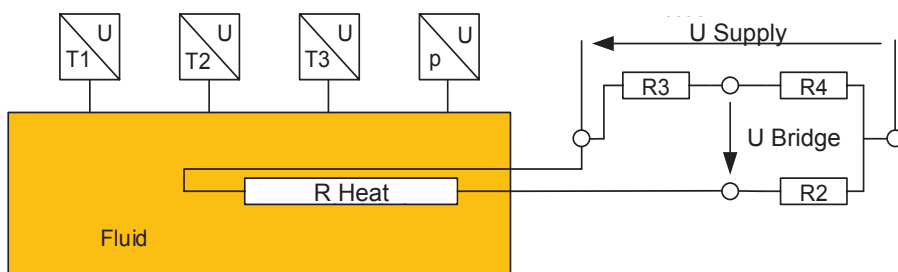


**Figure 6:** Schematic of the Wheatstone bridge used

The electric power provided to the oil can be calculated from the current and the heating wire resistance. While the current is known from the power-supply unit, the heating wire resistance is unknown and might even change with temperature. However, by using the Wheatstone bridge circuit the heating wire resistance can be deduced with help of three defined and temperature independent resistances. Two resistances in series are placed in parallel to a second set of resistances in series. One of these four resistances is the unknown one. By applying a voltage to the circuit a bridge voltage results from between the serial resistances of one set to the other. Now the unknown resistances can be calculated with (10) and (11). For this the resistances  $R_1$  to  $R_3$  need to be known. Additionally, these reference resistances need to be temperature independent. Otherwise the accuracy of the resistance calculation would be limited. **Figure 7** shows the final test rig setup.

$$U_{Bridge} = U_{Supply} \left( \frac{R_{Heat}}{R_{Heat} + R_2} - \frac{R_3}{R_3 + R_4} \right) \quad (10)$$

$$R_{Heat} = R_2 \frac{\left( \frac{U_{Bridge}}{U_{Supply}} + \frac{R_3}{R_3 + R_4} \right)}{1 - \left( \frac{U_{Bridge}}{U_{Supply}} + \frac{R_3}{R_3 + R_4} \right)} \quad (11)$$

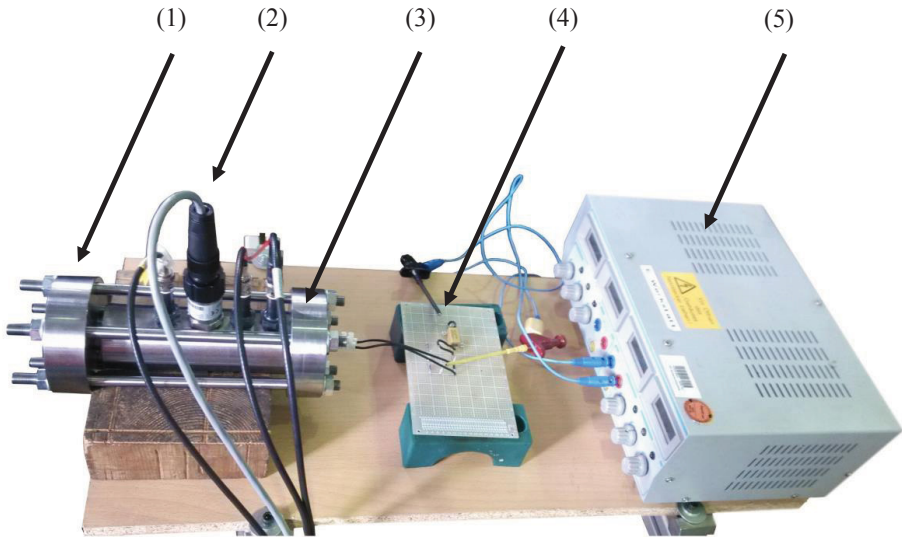


**Figure 7:** Test rig setup: (1) Lid with spring hook, (2) Sensors, (3) Measuring tube, (4) Wheatstone bridge with heat wire attached, (5) Power supply

#### 4. Calibration of Temperature Sensors

The temperature measurements are conducted using pt1000 sensors. In order to calibrate the sensor, several cooling cycles were run and the electrical resistance was measured with  $1/16 \, \Omega$  accuracy. The cycles were run using a oil reservoir on a laboratory hotplate with integrated stirrer to induce a homogenous temperature distribution in the fluid. Additionally the temperature was measured using a calibration thermometer. The results over all the cycles were evaluated and put into a table which translates the resistance into a temperature. Based on the acquired data, this allows to translate a difference of electrical resistance into a temperature difference.

#### 5. Results

To disregard convectional influences, the Rayleigh number is calculated using literature data for HLP46 at  $20 \, ^\circ\text{C}$ . The result shows a Rayleigh number of 214.65, due to  $Gr = 1362.03$  and  $Pr = 0.1576$ . Therefore, the convectional influences on the measurements can be neglected. Additionally, all the measurements were performed at a pressure level of 1 bar.

In order to measure the thermal conductivity of different oils, a calibration measurement was conducted. The calibration fluid was pure water with an electrical conductivity of less than  $1 \, \mu\text{S}/\text{cm}$ . The measurements were conducted at  $20 \, ^\circ\text{C}$ . **Table 2** shows the results compared with literature values. The different  $\lambda_i$ -values show the different combinations of temperature sensors used. The maximum deviation is 21.1 %. However, the deviation is in a tight band.

Fluid	$H_2O$ lit.	$H_2O$	Deviation [%]
$\lambda_1$	0.597	0.493	17.42
$\lambda_2$	0.597	0.500	16.24
$\lambda_3$	0.597	0.471	21.1

**Table 2:** Calibration Measurement for  $H_2O$

**Figure 8** shows the difference between every combination of sensors regarding their electrical resistance over time.  $\Delta R_{i,j}$  represents the difference between sensor  $i$  and  $j$ . The graph shows that an almost constant state is reached during the measurement. This state stays almost constant over 400 s. Therefore a quasi-static state is achieved with constant temperature differences over each sensor.



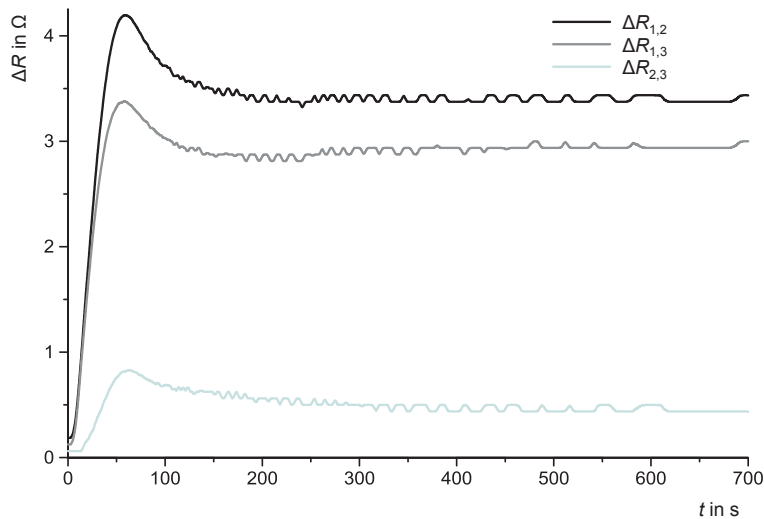


**Figure 8:** Difference of Resistances in a quasi-static state for HLP46

**Table 3** shows the measurement results for three different oils. The focus lies on the measurement of oils with the same viscosity index. Therefore, a viscosity index of 46 was chosen, because it represents a common class for many hydraulic applications. The measurements show, that HLP46 and HEES46 have very similar values for the first two temperature differences. Unfortunately,  $\lambda_3$  produces an offset for HLP and HETG oil. A possible explanation for this occurrence is that  $\lambda_3$  is calculated from the data of the two sensors closer to the wall. An influence of the wall on the sensors might cause this effect. Further investigations need to be done in order to determine the reason behind this phenomenon.

Oil	HLP46	HEES46	HETG40
$\lambda_1$	0.147	0.156	0.179
$\lambda_2$	0.161	0.157	0.183
$\lambda_3$	0.065	0.165	0.236

**Table 3:** Measurement Results for different oils

## 6. Conclusion and Outlook

In this paper, a short introduction into thermodynamic measurements is given. On basis of the first law of thermodynamics, an equation for the heat flux through a fluid is derived. One integral part of this equation is the thermal conductivity of the fluid. Little research has been done in order to determine those values for hydraulic oils. In order to generate a first understanding of the dimensions of the thermal conductivity of oils, a test rig was

designed to measure the thermal conductivity. The calibration of the temperature sensors was done by measuring the electrical resistance of the pt1000 elements used during several cooling processes. This way, the behavior of the sensors between each other was derived and can be used to measure temperature differences. Next, a calibration measurement with pure water was conducted. The maximum deviation was 21%. Additionally, three oils of a similar viscosity index were investigated.

The results show the tendency, that bio oil in general has a higher thermal conductivity than mineral oil. This impacts hydraulic applications as well as system simulations. The knowledge can be used to design smaller hydraulic tanks. If the thermal conductivity of the oil is higher, heat can be transferred out of the fluid faster. This reduces the idle time in a tank and therefore might reduce its size. The same is valid for heat exchangers.

System simulations always depend on accurate data in order to produce reliable results. If a simulation is used in order to design a whole hydraulic system, a good oil model is needed. Thermal properties play a vital role since isothermal conditions are a simplification of the system. Therefore, measuring the thermal conductivity of oil is a step towards a more holistic simulation approach.

In the future, more work has to be done in order to increase the accuracy of the measurements. Especially regarding the heating wire, power supply and temperature sensors. Additionally, investigations on high pressure states can be obtained by compressing the test tube and therefore generating a working pressure up to 400 bars. This can be done for a variety of oils and a database can be gathered.

## 7. References

- /1/ Witt, K., 1947. "Die Berechnung physikalischer und thermodynamischer Kennwerte von Druckflüssigkeiten, sowie die Bestimmung des Gesamtwirkungsgrades an Pumpen unter Berücksichtigung der Thermodynamik für die Druckflüssigkeit", Dissertation, University of Eindhoven
- /2/ Dalla Lana, E., De Negri, V.J., 2006. "A New Evaluation Method for Hydraulic Gear Pump Efficiency through Temperature Measurements", SAE Commercial Vehicle Journal, Paper Number 06CV-149
- /3/ Grigull, U., Sandner, H., 1990. "Wärmeleitung", 2nd edition, Springer Berlin Heidelberg, Berlin, Heidelberg
- /4/ Murrenhoff, H., 2014. „Fundamentals of Fluid power – Part 1: Hydraulics“, 7<sup>th</sup> Edition, Shaker, Aachen

/5/ Kneer, R., 2013. "Vorlesungsskript Wärme und Stoffübertragung I/II", Edition WS13/14, RWTH University Aachen

## 8. Nomenclature

$A_s$	Heat transfer area	$\text{m}^2$
$\bar{c}$	Average heat capacity	$\text{kJ}/(\text{kg K})$
$Gr$	Grashof number	
$\bar{h}_e$	Average external heat transfer coefficient	$\text{W}/(\text{m}^2 \text{K})$
$I$	Electric current	A
$L$	Length	m
$P$	Power	W
$Pr$	Prandtl number	
$p$	Pressure	bar
$p_F$	Surface pressure	$\text{N}/\text{mm}^2$
$Q$	Volume flow	$\text{l}/\text{min}$
$\dot{Q}$	Heat flow	W
$q''$	Heat flow density	$\text{W}/\text{m}^2$
$R$	Electric resistance	$\Omega$
$Ra$	Rayleigh number	
$r_{i/a}$	Radius, i: inner, a: outer	m
$\bar{T}$	Average temperature	K
$T$	Temperature	K
$U$	Electric voltage	V
$\bar{v}$	Average velocity	$\text{m}/\text{s}$

$\bar{\beta}$	Average coefficient of thermal expansion	1/K
$\delta$	Distance	m
$\Delta p$	Pressure difference	bar
$\Delta T$	Temperature difference between two points	K
$\eta$	Efficiency	
$\lambda$	Thermal conductivity	W/(m <sup>2</sup> K)